Proceedings of the Thirty-fourth (2024) International Ocean and Polar Engineering Conference **www.isope.org**
Rhodes, Greece, June 16–21, 2024

ISBN 978-1-880653-78-4; ISSN 1098-6189

Experimental Study of Influence of Bubble Flows on the Boundary Layer Below a Plate in Shallow Water Environment

*Qidi Gao, Jianhua Wang, Decheng Wan**

Computational Marine Hydrodynamics Lab (CMHL), School of Naval Architecture, Ocean and Civil Engineering,
Shanghai Jiao Tong University, Shanghai, China

*Corresponding author

ABSTRACT

In this paper, the influence of bubble flow on the flow field at the bottom of the plate is experimentally studied. In the experiment, PIV (Particle Image Velocimetry) is used to observe the complex flow field at the bottom of the plate in the circulating water tank. By using the pressure sensor to measure the flow force of the plate, the effect of different flow field conditions on the friction resistance of the plate surface is analyzed. The shallow water environment at different depths is simulated by changing the distance from the plate to the bottom by adding a cushion at the bottom of the circulating water tank. And an air-injection flat plate is specially designed to generate the bubble flow. Through the experimental results, the flow field of bubble flow on plate under different conditions was observed and analyzed. The change of bubble flow on the boundary layer of the plate will affect the friction resistance of the plate. And shallow water conditions will affect the bubble flow and further affect the bubble drag reduction.

KEY WORDS: Bubble Drag Reduction; Plate Experiment; Shallow Water Environment; Bubble Flow.

INTRODUCTION

Energy saving and emission reduction has been a hot topic in various industries in recent years. As the main form of freight transportation, the emissions of the shipping industry account for a large proportion of the total emissions. How to reduce the energy consumption in the shipping industry is the main research direction in the field of ship research. The direct way to reduce ship emissions is to reduce ship resistance, thereby reducing fuel consumption. It is difficult to break through the traditional drag reduction methods such as optimizing the ship ' s fluid shape, drag reduction structure and surface materials. Therefore, the bubble drag reduction method has become a feasible way to reduce ship resistance because its high efficiency and low cost.

The theory of bubble drag reduction has been studied for a long history. The earliest experiment produced bubbles by using electrolysis. When the wire wound on the axisymmetric body is energized, water will be electrolyzed to produce bubbles. When the bubbles form a bubble layer on the surface of the body, the surface friction resistance is obviously decreased (Michael, et al ,1973). The experiment proves that bubbles on the surface of the object can reduce the friction resistance. After that, many researchers have conducted various experiments on the bubble drag reduction since 1970s. Some researchers explore the mechanism of bubble drag reduction, while others study the factors that affect the drag reduction effect. Many experiments have proved the effectiveness of drag reduction. A special plate device was made and carried out experiments in a circulating water tank. The results showed that the optimal drag reduction effect could reach about 80 % (Madavan, et al ,1984). By comparing the drag reduction efficiency of bubbles on the upper and lower surface of the plate, it is found that the drag reduction effect is closely related to whether the bubbles are attached to the plate. This means that whether the bubble flow can flow along the plate surface will directly affect the drag reduction effect. Other than that, the drag reduction is caused by the change of effective viscosity in laminar boundary due to the decrease of density of mixed fluid (Marie, 1987; Lvov et al, 2005). The formation and movement characteristics of bubbles in drag reduction were observed by experiments. Through more plate experiments (Pal et al, 1988; Merkle et al, 1990), it is found that Only bubbles that can enter the inner layer of the boundary layer can have an effect on drag reduction, so in high Reynolds number flow, the boundary layer is thin, and it is necessary to use small enough microbubbles to achieve drag reduction. The drag reduction effect of bubbles in residence depends on the porosity near the wall (Janssen, et al ,1984). The coalescence and splitting of bubbles in the boundary layer is a mechanism to reduce the turbulence intensity in the turbulent boundary layer (Meng, et al, 1998). Shear deformation of bubbles along flow direction can reduce turbulence intensity in gas-liquid two-phase flow (Kitagawa, et al ,2004). It is found through experiments that the existence of bubbles changes the flow velocity field of the plate boundary layer, reduces the shear resistance between the fluids in the boundary layer, and inhibits the flow turbulence, thereby reducing the friction resistance (Ferrante, et al ,2004). Experimental study on drag reduction mechanism such as Madavan (1984); Merkle (1992); Tanaka (2021) and Murai (2020) proved some possible drag reduction mechanism. A 50-meter-long plate experiment by Takahashi (2003) verified the influence of injection position on bubble drag reduction. After that, Gao (2023) has proved that turbulence suppression is one of the important mechanisms of bubble drag reduction through a series of plate experiments.

Due to the complexity of bubble drag reduction, more and more researchers have begun to try to reveal the mechanism of drag reduction by numerical simulation. Kanai (2001) through the direct numerical simulation of the interaction between the two bubble flow and the boundary layer, proved that the main influencing parameters are Weber number and Froude number. According to the Euler two-phase flow model, the bubble drag reduction is numerically calculated and the details of the boundary layer are simulated (Kunz, et al, 2007). Hoang (2011) combines the boundary layer integral equation and empirical formula to calculate the bubble reduction for the real ship. The turbulence change in the boundary layer is considered in the calculation method, which is suitable for the calculation of bubble drag reduction in real ship scale. Zhang (2020) uses Euler–Lagrange method to study the bubble drag reduction in turbulent channel flow and boundary layer flow. The results show that the drag reduction is directly related to the migration of bubbles away from the wall.

Up to now, both physical experiments and numerical simulations have shown that bubble drag reduction is a very complex physical process, and its drag reduction mechanism is intermixed and influenced by each other. Although the mechanism of drag reduction is not clear, the influence of bubble flow on the boundary layer has been proved to be one of the important mechanisms of bubble drag reduction. Therefore, this paper will try to illustrate the flow field and boundary layer of flat bubble flow through PIV by flat plate experiment, and analyze the change of plate boundary layer caused by bubble flow in shallow water environment.

EXPERIMENTAL FACILITY

The experiment was carried out in a circulating flume of Zhejiang Ocean University, as shown in Fig. 1. The water tank is 20 m in length, 0.5 m in width and 0.6 m in height. The flow-rate range is 0 L/s to 100 L/s and the theoretical flow velocity is 0 m/s to 0.75 m/s.

Fig. 1. The circulating water tank

The experimental plate size is 400 * 120 * 8 mm, the flat plate is made of aluminum and the surface of plate is smooth. A rectangular groove on the upper surface at a certain position from the front end of the plate (incoming flow direction) is carved. The groove is 12 mm in width and 3 mm in depth. The groove acts as a connection part between the plate and the air chamber. With a special rubber gasket, the air tightness of injection is guaranteed. The air chamber is 120 mm in length, 12 mm in width and 10 mm in height, connected to the plate by two bolts. The upper part of the air chamber is connected with the air supply pipe by a threaded hole, as shown in Fig. 2 (b). On the plate, there are 11 air holes with the diameter of 1 mm. Defining *a* (mm) as the distance from the air holes to the front end of the plate. The plate is shown in Fig. 2.

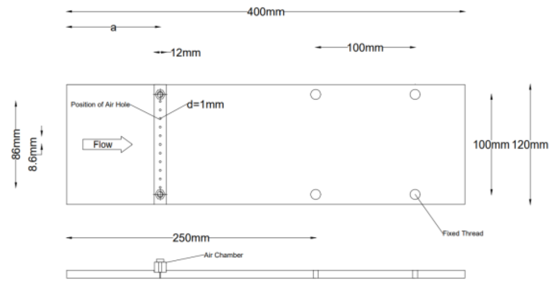

(a) The top and side views of the flat plate

(b) The flat plate

Fig.2 The experimental flat plate

A gasket is added between the air cavity and the flat air groove to ensure the sealing of the device. The upper part of the air chamber is connected with the flow meter and the regulating valve through the gas supply pipe and finally connected to the air compressor for the flat air supply. The plate is connected to the fixed bracket on the sink through four holes arranged behind it. The guide rail is connected to the upper part of the support, and the guide rail can move in a single degree of freedom along the flow direction. When the plate is forced in the water, the four supports will move synchronously, and the slider on the guide rail will move backward as shown in Fig. 3. The back end of the slider is connected with the fixed pressure sensor, and the plate force is directly measured by transmission.

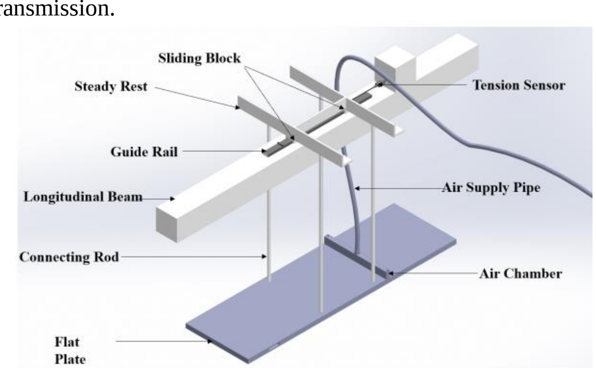

(a) The design model

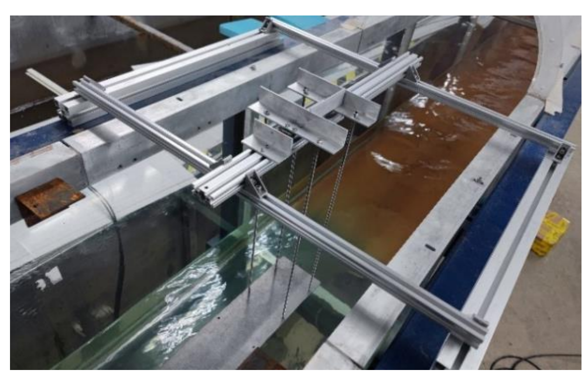

(b) Actual test equipment

Fig. 3 The design and actual model of the experimental installation

Because the plate is connected to the connecting rods, and the air chamber with a part of air pipe is under the water flow in the experiment. The force measured by the tension sensor is the sum of the forces, including the frictional resistance and the inertial forces of plate, connecting rods, air chamber and air pipe. However, in the experiment, all experimental devices are the same under the same conditions. The only distinction is injecting air or not, which determines the friction resistance of the flat plate. Therefore, in order to research the effect of reducing friction resistance of the plate caused by bubble flow, we define F_0/F as the force ratio of the plate. Which the F0 means the total force with air injection, and the F means the total force without air injection. The smaller the value of the F_0/F, the smaller the friction resistance on the plate. On the contrary, the worse the drag reduction effect is. The PIV system is shown in Fig. 4, including the laser device, high-speed camera and control host. The tracer particle was used to reflect the laser, which the density is almost the same as that of water, and the particle size is 10 μm. An air compressor is used as the air supply, the volume of the air storage tank is 30 L The air flow rate is measured using a gas flowmeter with measuring range of 0 L/min to 45 L/min.

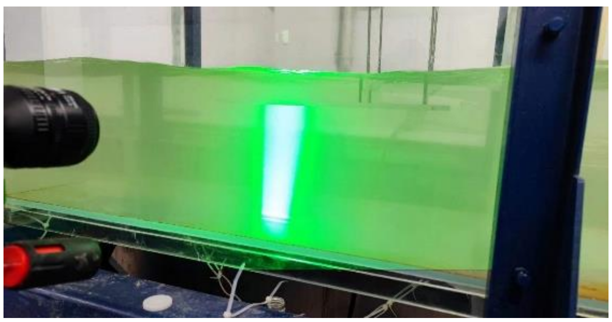
(a) The laser device


(b) The high-speed camera

Fig. 4. The PIV system and tracer particle

Fig. 5 shows the 2-D schematic diagram of the experiments of the flat plate. A shallow water cushion is added at the bottom of the flume and under the flat plate to simulate shallow water environments. In the experiment, different shallow water depths are simulated by changing the height of the shallow water cushion. In the experiment, H is defined as the distance between the bottom of the plate and the shallow water cushion to represent different shallow water levels as shown in Fig. 6 and three different H conditions were set up in the experiment as 40 mm, 70 mm and 100 mm. The injection position is represented by a which means the distance between the front end of the plate and air holes. In the experiment, 10 different a values are set, 40 mm, 50 mm, 60 mm… 130 mm. The air flow rate is 3 L/min, 6 L/min, 9 L/min… 30 L/min, and the flow velocity is 0.32 m/s, 0.42 m/s, 0.52 m/s, 0.62 m/s, 0.72 m/s, represented with v.

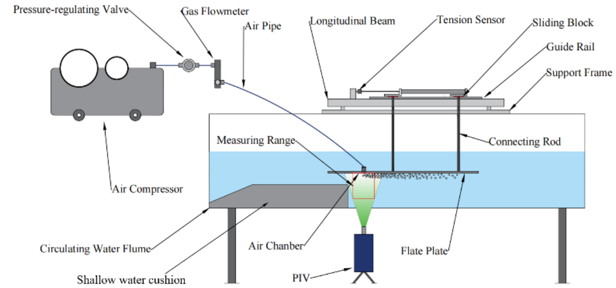

Fig. 5 The 2-D schematic diagram of the experiments of the flat plat

EXPERIMENT

The experimental schemes are summarized in Table 1. In the experiment, each a condition uses a plate with the same size but different air holes positions. Each plate was tested at 5 different flow velocity, 3 different H and 10 different air flow rates. The flow field of the plate and the force of the plate were recorded respectively.

Table 1. Experimental schemes

a （mm）	Flow velocity （m/s）	H (mm)	Air flow rate （L/min）
40	0.32	40	3
50	0.42	70	6
60	0.52	100	9
70	0.62		12
80	0.72		15
90			18
100			21
110			24
120			27
130			30

Due to the large number of flow field conditions observed by PIV in the experiment, only some typical conditions are analyzed. Fig. 6 shows the velocity contours of the flow field at different H on the lower surface of the plate in the non-jet state when the incoming flow velocity is 0.72 m/s and 0.52 m/s, respectively.

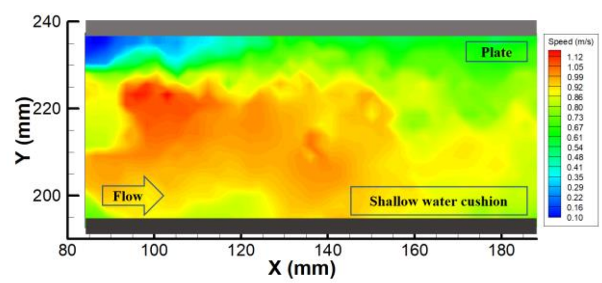

(a) v=0.72 m/s, H =40 mm

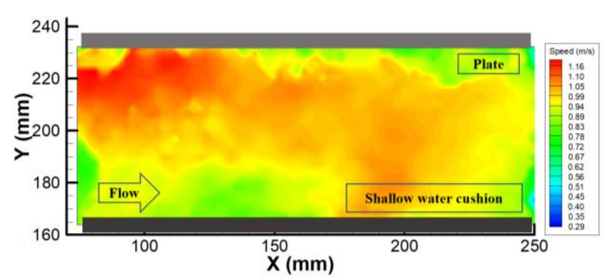

(b) v=0.72 m/s, H =70 mm

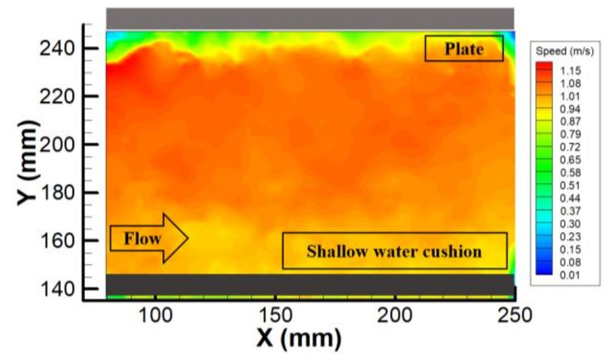

(c) v=0.72 m/s, *H* =100 mm

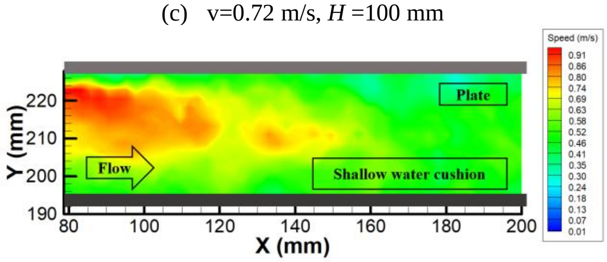

(d) v=0.52 m/s, *H* =40 mm

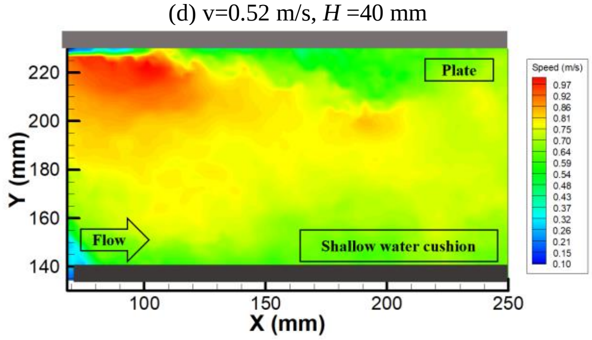

(e) v=0.52 m/s, *H* =70 mm

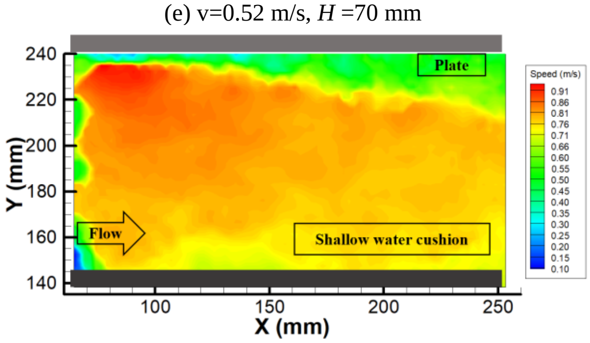

(f) v=0.52 m/s, *H*=100 mm

Fig. 6 Velocity contours of plate flow field in shallow water environment

Fig. 7 shows the results of the tests with a = 80 mm, air flow rate is 15 L/min, flow velocity is 0.52m/s, three shallow *H* velocity contours results. Fig. 8 shows the velocity contours of 5 flow velocities when the *H* is 40 mm, a is 80 mm, air flow rate is 15 L/min.

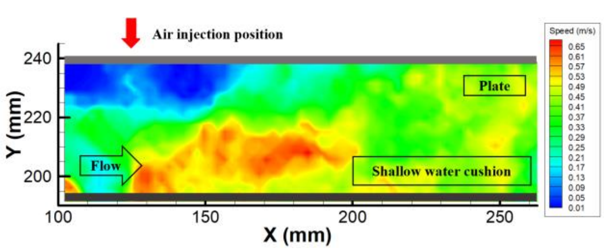

(a) H=40 mm

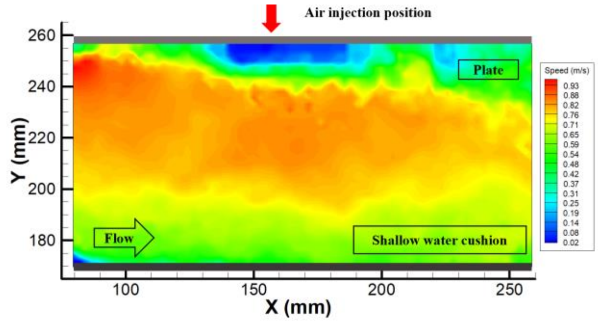

(b) H=70 mm

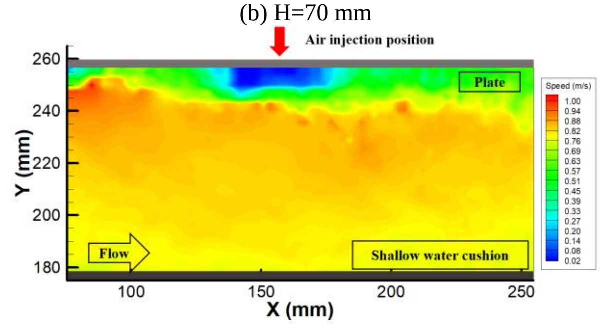

(c) H=100 mm

Fig. 7 Velocity contours with injection, *a*=80mm, air flow rate is 15L/min, flow velocity is 0.52m/s.

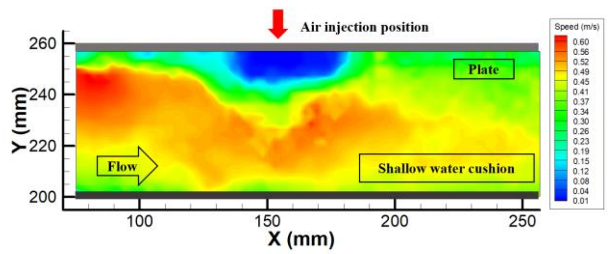

(a) v=0.32 m/s

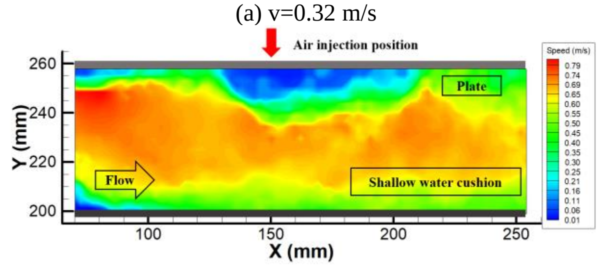

(b) v=0.42 m/s

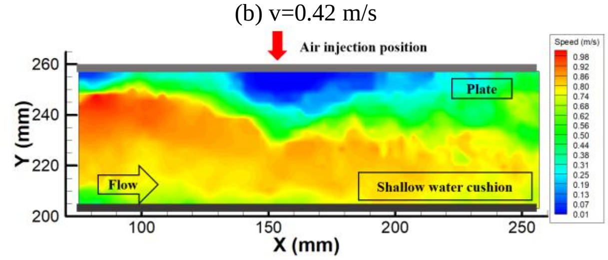

(c) v=0.52 m/s

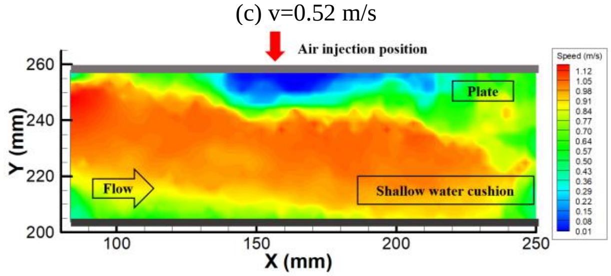

(d) v=0.62 m/s

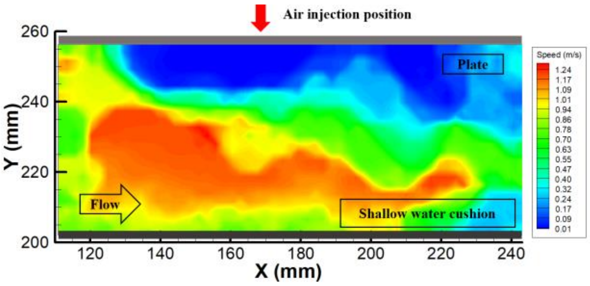

(e) v=0.72 m/s

Fig. 8 Velocity contours with injection, *a*=80 mm, air flow rate is 15 L/min, H=40 mm.

EXPERIMENTAL RESULT

Flow Field of Plate

It can be seen from the Fig. 6 that in the case of a certain flow velocity, the flow velocity in the shallow water area is significantly greater than the average flow velocity, and the flow velocity changes sharply. The smaller the shallowness, the greater the change of flow velocity, and the greater the flow velocity in the shallow water area. On the contrary, the flow velocity changes little, and the flow velocity in the shallow water area increases less than the former. The turbulence of the flow field in the shallow water area is strong, and the turbulence of the lower surface of the plate increases. Compared with the non-shallow water environment, due to the effect of the turbulent flow field at the bottom of the water body, the flow field state of the plate itself is disturbed, forming a more disordered turbulent state, the local velocity is uneven, the flow direction is uncertain, and the turbulent flow is obvious.

The bubbles will significantly change the flow field on the lower surface of the plate. It can be seen from the Fig. 9 that before the injection, a part of flow field of plate is already in turbulent state. In front of the air holes, the boundary layer is thin and the near wall velocity is higher than mean velocity. After the injection, the bubble flow is still formed as before, so that the subsequent flow field maintains the boundary layer state of the bubble flow. However, the turbulence is already forming ahead, causing the bubble flow to be affected by it. In this injection position, the boundary layer of bubble flow is thinner and the flow velocity in the boundary layer is higher.

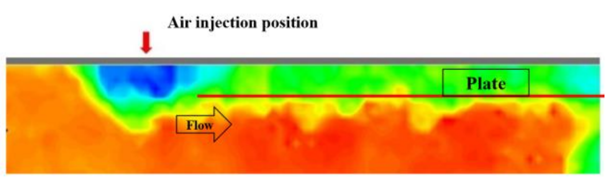

Fig. 9 Velocity contours when *a*=80 mm, air flow rate is 15 L/min

When *H* is changed, it can be seen from Fig.7 that the bubble can also have a significant effect on the lower surface flow field of the plate. As with the non-shallow water environment, the bubble can significantly change the turbulence phenomenon of the plate, which is manifested in the formation of bubble flow on the lower surface of the plate, and the thickness of the bubble flow boundary is thicker than that of the original turbulent boundary layer. The flow velocity in the boundary layer is lower and can maintain a stable distance. The influence of the bubbles on the flow field of the plate is related to the shallowness *H*. When *H* decreases, the water flow velocity increases, and the suppression effect of the air curtain on turbulence becomes weaker, which is manifested by the decrease of the thickness of the bubble flow boundary layer, the increase of the flow velocity in the boundary layer, and the blurring of the boundary layer boundary line. On the contrary, when *H* increases, the effect of air curtain is more obvious, which is similar to the flow field in non-shallow water environment. The flow field at the bottom of the water body will damage the bubble flow boundary layer, and this effect will increase with the decrease of *H*. When *H* decreases, the bubble flow boundary layer is disturbed by the bottom flow field, and it is more difficult to maintain a stable flow state, and the continuous range of the boundary layer becomes smaller.

When only changing the incoming flow velocity, the effect of the air curtain on the flat flow field in shallow water environment is basically the same as that in non-shallow water environment. It can be seen from the Fig .8 that the increase of flow velocity will make the turbulent flow effect of the plate and the bottom of the water body more intense. Because the position of the shallow water cushion is closer to the front of the plate, a turbulent flow field has been formed at the bottom of the water body under the front of the plate. As the incoming flow velocity increases, the turbulence intensity increases, and the influence of the flow field at the bottom of the water body on the flat plate flow field gradually becomes stronger. Under such influence, the bubble flow boundary layer is difficult to maintain a long distance. In practice, it will dissipate at a faster speed, and the flat flow field will be restored to the turbulent flow field.

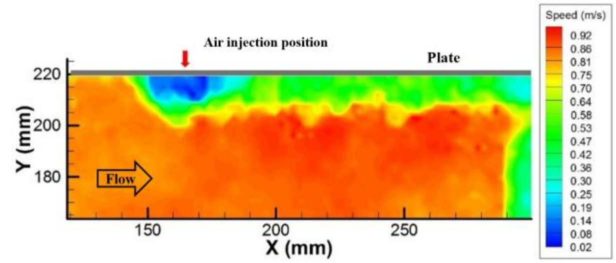

Fig. 10 Velocity contour with injection, *a*=80 mm, air flow rate is 15 L/min, flow velocity is 0.52 m/s, non-shallow water environment

Comparing Fig. 7 (a) and Fig. 10, it can be clearly seen that when the injection position, incoming flow conditions and the air flow rate are the same, the distance of the bubble flow under the flat plate in the shallow water environment is significantly shorter than that in the non-shallow water environment. This is due to the turbulence of the shallow water flow field affecting the bubble flow on the lower surface of the plate. The original stable bubble flow diffuses rapidly under the influence of bottom turbulence, which shows that the thickness of the boundary layer of the bubble flow decreases, the velocity in the boundary layer increases, and the drag reduction effect decreases.

Drag Reduction Efficiency

As for the drag reduction efficiency, it can be analyzed by comparing F_0/F under different working conditions. Fig. 11 shows the resistance ratio by F_0/F under different *H*.

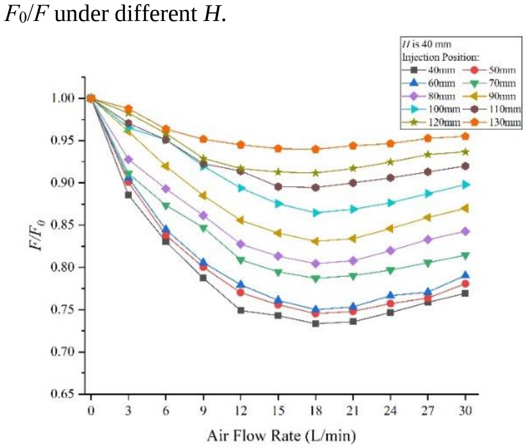

(a) *H* is 40 mm

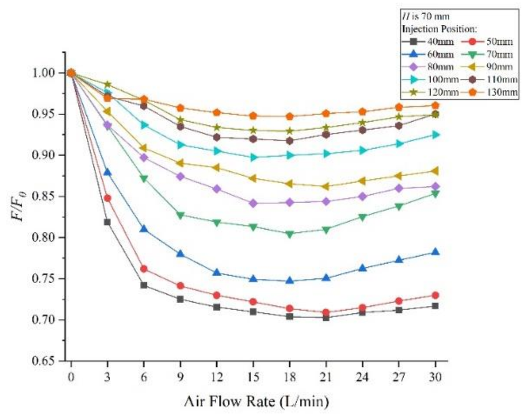

(b) *H* is 70 mm

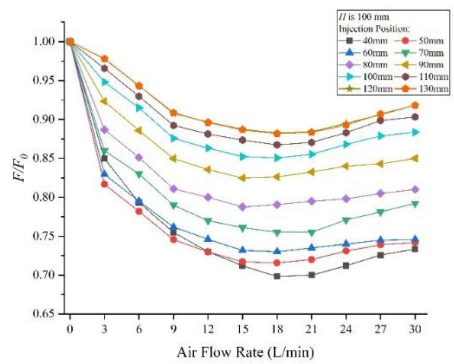

(c) *H* is 100 mm

Fig. 11 The resistance ratio F_0/F of different H

By comparing the experimental results, it can be found that in the shallow water environment, the effect of bubbles on the reduction of plate resistance is similar to that in the non-shallow water environment. With the increase of jet volume, the drag reduction effect shows a trend of increasing first and then decreasing. However, different from the non-shallow water environment, in the shallow water environment, when the jet volume exceeds the optimal jet volume, the reduction trend of drag reduction effect is gentler. Different injection positions still have a significant effect on the drag reduction effect, but this effect can be reflected by the change of H in shallow water environment. For example, in Fig. 11 (a), when the H is 40 mm, the F_0/F increases significantly from 60 mm to 70 mm. In Fig. 11 (c), the H is 100 mm, and the F_0/F changes greatly after 80 mm. The reason is that the decrease of shallowness increases the incoming flow velocity below the plate. Although the flow velocity of the external flow field is the same, due to the influence of shallow water on the flow velocity, F_0/F appears similar to the phenomenon when the flow velocity increases. With the increase of H, the variation of F_0/F value tends to be more non-shallow water environment. Because when the H increases, the influence of the bottom of the water body on the flow field of the lower surface of the plate gradually becomes smaller, and the bubble flow as a stronger external intervention reason, the effect is further strengthened, so that the flow field influence of the shallow water environment is weakened, so the drag reduction effect shows a trend similar to that of the non-shallow water environment.

The influence of shallow water environment on the flow field of the plate is mainly through two aspects. One is to increase the flow velocity below the plate. Under this action, the change of the velocity of the flow field under the flat plate is similar to the change of the velocity of the pure flow field in the non-shallow water environment, and the turbulent transition position of the flat plate is forced to advance. Therefore, in the shallow water environment, at the same external flow velocity, it is necessary to advance the injection position to achieve the effect of turbulence suppression on the flat plate. The shallow water environment also affects the flow field on the lower surface of the plate through the turbulence at the bottom of the water body. Because the bubble flow is disturbed by the shallow water flow field, the effect of the air flow rate on the drag reduction effect is stronger than that of the non-shallow water. With the increase of the air flow rate, the drag reduction effect does not decrease rapidly after reaching the maximum, but decreases at a slow speed. Compared with the result of too large air flow rate in non-shallow water environment, the large air flow rate in shallow water can also achieve better drag reduction effect.

CONCLUSIONS

In this paper, the drag reduction of bubble flow in shallow water environment is studied experimentally. Through the observation of the plate flow field, the influence of shallow water flow field on the plate flow field is studied. At the same time, the drag reduction effect of the bubble flow on the flat plate in the shallow water flow field and the influence of the shallow water flow field on the boundary layer of the bubble flow are studied. Finally, the following conclusions are drawn.
The most intuitive influence of the shallow water environment on the flow field below the flat plate is to change the flow velocity of the water flow below the flat plate. At the same average flow velocity, the flow velocity increases significantly after passing through the shallow water environment, and the original turbulence transition position of the flat plate is changed due to the increase of velocity. Compared with the non-shallow water environment, the turbulent transition position of the plate is more forward.

In the shallow water environment, the turbulent flow field at the bottom of the shallow water will affect the flow field on the lower surface of the plate, and then affect the turbulent boundary layer of the plate. The flow field of the two will be mixed and interacted with each other, which will make the flow field more disordered and increase the resistance of the plate. The factors affecting the drag reduction effect in shallow water environment are slightly different from those in non-shallow water environment. Due to the complex interaction between the shallow water flow field and the flat flow field, the influence of the injection position on the drag reduction effect is weakened. Due to the increase of flow velocity and the uneven flow field, the effect of air flow rate is strengthened. And it can still achieve better drag reduction effect when the air flow rate is large.

The bubble flow at the bottom of the flat plate will change the original boundary layer structure and form a flow state of the bubble flow boundary layer. The thickness of the bubble flow boundary layer is significantly larger than that of the single-phase flow turbulent boundary layer, and the velocity in the boundary layer is lower. Under the action of bubbles, the turbulent vortex structure in the boundary layer of bubble flow would obviously be suppressed, the vorticity is presumably reduced, and the flow is becoming more stable, and the drag reduction effect is produced.

For the future studies, the Reynolds-averaged analysis of the flow field, such as average velocity, contours, turbulence intensity contours, etc. will be used to process the experimental results. It is of great significance for the study of bubble drag reduction. Moreover, the effect of bubble size on reduction will be studied.

ACKNOWLEDGEMENT

This work is supported by the National Natural Science Foundation of China (52131102), to which the authors are most grateful.

REFERENCES

Ferrante, A and Elgobashi, S (2004). “On the physical mechanisms of drag reduction in a spatially developing turbulent boundary layer laden with microbubbles,” Inter. Fluid Mech, 503(3),45-55.
Gao, QD, Lu, JS, Zhang, GL, Zhang, JW, Wu, WF and Deng, JJ (2023). “Experimental study on bubble drag reduction by the turbulence suppression in bubble flow,” Ocean Engineering, volume 272, 15 March 2023, 113804.
Hoang, C, Yasuyuki, T and Yugo, S (2011), “A consider on drag reduction by air lubrication using integral type boundary layer computation,” The Japan Society of Naval Architects and Ocean Engineers, 2011(6), 59-65.
Janssen, LJJ, Sillen, CW and Barendrecht, E (1984). “Bubble behavior during oxygen and hydrogen evolution at transparent electrodes in solution,” Electrochimica Acta, 29(5), 633-642.
Kanai, A and Miyata, H (2001), “Direct numerical simulation of wall turbulent flows with microbubbles,” International Journal For Numerical Methods In Fluids, 35, 593-615.
Kitagawa, A, Hishida, K and Kodama, Y (2004). “Two phased turbulence structure in a microbubble channel flow,” Proc. of 5th Symp. on Smart Control of Turbulence, Tokyo 2004.
Kunz, RF, Gibeling, HJ and Maxey, MR (2007), “Validation of two-fluid Eulerian CFD modeling for microbubble drag reduction across a wide range of Reynolds numbers,” Journal of Fluids Engineering, 2007(129), 66-79.
Lvov, VS, Pomyalov, A and Procaccia, I (2005). “Drag reduction by microbubble in turbulent flows: the limit of minute bubbles,” Phys. Rev. Lett. 94, 174502.
Madavan, NK, Deutsch, S and Merkle, CL (1984). “Reduction of turbulent skin friction by microbubbles,” Physics of Fluids, 1984 (2), 356-363.
Marie, JL (1987). “Simple analytical formulation for microbubble drag reduction,” Physics Chemical Hydrodynamics, 8(2), 213-220.
Meng, JCS and Uhlman, JS (1998). “Microbubble formation and splitting in a turbulent boundary layer for turbulent reduction,” Proc. Int. Symp. Seawater Drag Reduction., Newport, Rhode Island, 1998, 341-55.
Merkle, C (1990). “Drag reduction in liquid boundary layers by gas injection,” Prog. Astronaut. Aeronaut, 1992 (123),351-412.
Michael, E, McCormick and Rameswar, B (1973). “Drag reduction of a submersible hull by electrolysis,” Journal of Naval Engineers, 85(2), 11-16.
Murai, Y, Sakamaki, H, Kumagai, I, Park, HJ and Tasaka, Y (2020). “Mechanism and performance of a hydrofoil bubble generator utilized for bubbly drag reduction ships,” Ocean Engineering, Volume 216, 15 November 2020,108085.
Pal, S, Deutsch, S and Merkle CL (1989) “A comparison of shear stress fluctuation statistics between microbubble modified and polymer modified turbulent flow,” Physics of Fluids, 1989, 1360-1362.
Pal, S, Merkle, CL, and Deutsch, S (1988). “Bubble characteristics and trajectories in a microbubble boundary layer,” Physics of Fluids, 31(4), 744-751.
Tanaka, T, Oishi, Y, Park, HJ, Tasaka, Y, Murai, Y and Kawakita, C (2021). “Repetitive bubble injection promoting frictional drag reduction in high-speed horizontal turbulent channel flows,” Ocean Engineering, volume 239, 1 November 2021, 109909.
Takahashi, T, Kakugawa, A, Nagaya, S, Yanagihara, T and Kodama, Y (2003). “Mechanisms and scale effects of skin friction reduction by microbubbles,” J. Kansa Soc. N. A. Japan, 2003(239),1-9.
Zhang, XS, Wang, JH and Wan DC (2020), “Euler–Lagrange study of bubble drag reduction in turbulent channel flow and boundary layer flow,” Physics of Fluids, 32, 026101.